RUBBLE MOUND BREAKWATER STABILITY WITH MULTIDIRECTIONAL WAVES

Max CANEL*, Arthur de GRAAUW*

-

ABSTRACT

This paper gives a short description of a three-dimensional physical model study of the effects of directional spreading of random waves on the stability and overtopping of a rubble mound breakwater. The model consists of a conventional breakwater with four different types of armour (rock, Tetrapod blocks, grooved Antifer cubes and ACCROPODE® blocks). It concludes that armour stability generally increases with increasing directional spreading but some noticeable features concerning oblique multidirectional waves lead to renewed prudence in the design of coastal structures.

1. INTRODUCTION

A three-dimensional physical model study of the effects of directional spreading of random waves on the stability and overtopping of a rubble mound breakwater was performed in the 30 x 40 x 1 m wave basin recently built in Grenoble (France).

The model (scale 1:50) consisted of a conventional breakwater with four different types of armour : rock, Tetrapod blocks, grooved (Antifer) cubes and ACCROPODE® blocks.

This study was performed in parallel with a study at LNH (EDF, Chatou, France) where a similar model (scale 1:60) was used to check the stability of the same four types of block with monodirectional waves from various incident directions.

This study was carried out as part of a cluster of projects called "G6 Coastal Structures" (G6 - S) within the framework of the EC Marine Science and Technology Programme (MAST-1). It was led by the "Group of Six" (G6) formed by the major European hydraulics laboratories involved in coastal engineering research.

The overall objective was to provide the technical basis for the preparation of European Guidelines on the design of coastal structures which were scheduled to be drawn up in subsequent programmes.

* SOGREAH Ingénierie, Grenoble (France)

2. EXPERIMENTAL SET-UP

2.1 MODEL LAYOUT

The breakwater was straight over a distance of 15 m including both roundheads.

The model was built on a horizontal bottom at a water depth of 0.54 m and angled at 15° with respect to the wave generator in order to be able to generate waves at 45° with respect to the breakwater without having an angle larger than 30° with respect to the wave generator (Figure 1).

The segmented wave generator consists of 60 paddles, each 0.50 m wide and 1.4 m high. Each paddle is individually driven in translational motion by a hydraulic actuator. The control signal is generated using the technique of white noise filtering following Guilbert and Huntington (1991) or by adding sinusoidal components. The maximum wave heights are : H_s = 250 mm and H_{max} = 400 mm for a JONSWAP spectrum and a peak wave period T_p = 2.2 s.

2.2 BREAKWATER CROSS-SECTION

A realistic cross-section was chosen as shown in Figure 2, leading to a considerable volume of about 10 m^3 of carefully selected and sieved materials.

The breakwater was subdivided into four sections of 3 m in which four different types of block were used for the armour layer.

Block	ROCK	TETRAPOD blocks	Grooved CUBES	ACCROPODE® blocks
M_{50} (g)	192	114	87	74
ρ (g/cm^3)	2.65	2.41	2.42	2.36
ΔD_n (mm)	69	51	47	43
Number (N1)	488	463	764	462
Cotg α	3/2	4/3	4/3	4/3

The median mass (M_{50} is exceeded by 50% of the blocks) and the density (ρ) were measured on a representive sample of each type of block. The traditional definitions of the relative buoyant density (Δ) and the nominal diameter (D_n) were used :

$$\Delta = \frac{\rho_s - \rho_w}{\rho_w}$$ with ρ_s and ρ_w respectively the density of blocks and of water

$$D_n = (\text{volume of block})^{1/3}$$

All types of block, except ACCROPODE®, were placed in two layers.

The number of blocks given above concerns the central part of each section (1.2 m out of the 3 m available for each type of block) where damage was observed during the test.

The number of blocks was about 450-500, except for cubes, where more than 750 blocks were placed. This was due to their rather small size compared to rock and Tetrapod blocks. It may be noted that the rather small number of ACCROPODE® blocks, compared to the number of cubes, is of course due to the ACCROPODE® single layer technique.

The slopes were set at 1:1.33 except for rock, where a slope of 1:1.5 was chosen.

The block sizes were defined from preliminary tests performed at SOGREAH and LNH. They were chosen in such a way that they would start to be unstable at roughly the same significant wave height without leading to unrealistic block sizes at the 1/50 scale : the 9 ton ACCROPODE® is close to the lower limit of normal use of that block and the 24 ton rock is well above the normal sizes available at reasonable cost from quarries.

2.3 TEST PROGRAMME

The objective was to investigate the effect of both directional spreading and wave obliquity on the stability and overtopping of the breakwater. The following 7 tests (A to G) were performed :

θ	0°	30°	45°
$\sigma = 0°$	A	(see LNH)	
$\sigma = 10 - 15°$	B - C - D	-	-
$\sigma = 20°$	E	G	F

With :

θ Mean incident wave direction with respect to breakwater

σ Mean directional spreading (standard deviation)

Hence, test A with monodirectional waves ($\sigma = 0°$) was used as a reference and as a comparison with results obtained at LNH.

Tests B, C and D were meant to investigate a "normal" directional spreading with frontal wave incidence.

Tests E, F and G were meant to investigate a "wide" directional spreading with various wave incidences.

Obviously, test results were meant to be grouped to investigate both the effect of directional spreading (tests A, B-C-D, E) and the effect of wave obliquity (tests E, F, G).

Each test consisted of a series of 8 steps of about 1 800 waves (actually measured during tests : 1 750 to 2 100) with increasing wave height and a constant wave steepness of about $S_{op} = H_s/L_{op}$ = 3.8% (actually measured during tests : 3 to 5%). The following target values were defined so that SOGREAH and LNH would work on comparable cases :

Step	1	2	3	4	5	6	7	8
T_p (s) H_s (mm)	0.78 36	0.95 54	1.09 72	1.23 90	1.34 108	1.45 126	1.54 144	1.64 162

A large number of preliminary tests was performed to obtain the settings required for the above desired wave conditions.

All tests were performed with a JONSWAP spectrum combined with Mitsuyasu-type spreading functions :

$$S'(f, \theta) = S(f) \,.\, D(f, \theta)$$

where S(f) typically is a JONSWAP spectrum and D(f, θ) is given by Mitsuyasu (1975) :

$D(f, \theta) = \cos^c \theta/2$

c $= 23\, \bar{f}_p^{\,-2.5}\, (f/f_p)^b$

$\bar{f}_p$ $= 2\, \pi\, f_p\, U/g$

b $= 5$ when $f \leq f_p$; and -2.5 when $f \geq f_p$

U = wind speed (m/s)

Hence, the Mitsuyasu spreading function yields a spreading depending on the wave frequency f with a minimum spreading at the peak of the spectrum ($f = f_p$).

It may be noted that the Mitsuyasu formulation includes a θ/2 angle instead of θ as used in the $\cos^{2n} \theta$ formulation. However, it appears that $\cos^a \theta \approx \cos^{4a} \theta/2$ (for $a \geq 3$ and $\theta \leq 85°$).

2.4 MEASUREMENTS

Offshore waves were measured by means of a special probe in which a wave height gauge is combined with point measurement of two perpendicular orbital velocity components in the horizontal plane (Sand and Mynett, 1987). The directional wave spectrum was determined from an analysis using the Maximum Entropy Method (Nwogu et al, 1987).

In addition, a statistical analysis of wave heights and periods from all directions was carried out using the signal of the offshore wave height gauge. **The value of $H_{1/3}$ resulting from this statistical analysis was used as a reference for all tests** (H_s).

Damage was observed in the central part of each section (1.2 m out of the 3 m) after each step of approx. 1 800 waves. The armour layer consisting of rock was painted with several colours (band width of 2 D_n) in order to be able to count the number of blocks fallen or shifted. The other types of block were counted in a similar way. Photographs were also taken in order to be able to superimpose pictures.

Overtopping was observed in the middle of each section by counting the number of overtopping waves by means of a set of electrodes placed just behind the top of the crown wall.

2.5 HOMOGENEITY OF WAVE FIELD

Due to reflexions from the breakwater and on the side walls and wave paddles, the wave field in the basin need not be homogeneous. However, extensive absorbing beaches on both sides of the basin and the choice of the location of the multidirectional wave gauge (see Figure 1) helped to minimize the problem.

Measurements with a three-wave-gauge array (enabling a distinction between incident and reflected waves) placed successively in front of each of the four sections during test A with frontal waves showed that nearshore incident waves were close to the offshore measured values and close to each other :

$$H_{1/3} \text{ nearshore incident} / H_s = 0.94 \text{ to } 1.04$$

It was thus concluded that the significant wave height along the breakwater was homogeneous within a ±5% range.

Further comparisons of several wave height analyses at the offshore location also showed some consistent results throughout the complete series of tests with multidirectional waves :

- For H_{mo} deduced from a spectral analysis without distinction between incident and reflected waves :

$$H_{mo} \text{ offshore incident + reflected} / H_s = 0.99 \text{ to } 1.04$$

- For H_{mo} deduced from a spectral analysis including the distinction between incident and reflected waves :

$$H_{mo} \text{ offshore incident} / H_s = 0.94 \text{ to } 1.01$$

- For H_{mo} deduced from a spectral analysis and after removal of the breakwater from the basin :

$$H_{mo} \text{ without structure} / H_s = 0.90 \text{ to } 0.98$$

It was thus concluded that the chosen offshore reference wave height H_s was an acceptable representation of the wave field within a range of ±5 to 10%.

3. TEST RESULTS

3.1 ARMOUR STABILITY

After each of the 8 wave height steps the number of displaced blocks was counted (blocks fallen down the slope and blocks shifted out of a $2D_n$ band width).

Damage to the armour was not restored after each step, so that the damage was cumulated as it would be during a single storm in prototype.

The number of displaced blocks (Nd) was related to the total number of blocks (N1) and expressed as a percentage in Figures 3 to 6. Each figure concerns one type of block and contains two graphs. One graph gives the results for tests A, B, C, D, E, that is for $\theta = 0°$ and $\sigma = 0°, 10°, 15°, 13°$ and $21°$ respectively, hence combining results for various directional spreadings with frontal waves. The second graph gives the results for tests E, G, F (and A as a reference), that is for $\sigma = 19 - 21°$ and $\theta = 0°, 30°, 45°$ respectively, hence combining results for various wave incidences with a wide directional spreading.

It should be stressed that the important factor is the position of the points. The connecting lines may give a wrong impression of the variation in stability with increasing wave height.

For the first group (A, B, C, D, E), the following general trend can be seen for all types of block:

. Test A yields the most unstable situation;

. Test E yields the most stable situation (with an exception for Tetrapod blocks);

. Tests B, C, D yield intermediate stability.

For the second group (E, G, F), it can be seen that:

. Test A yields the most unstable situation;

. Test E yields the most stable situation;

. Tests G, F yield intermediate stability.

Furthermore, for frontal waves (test A), all types of block correspond quite closely to van der Meer's estimates for critical values of $H_s / \Delta D_n$:

Block	Start of damage	Failure
ROCK	1.5 (S = 2)	2.0 (S = 8.0)
TETRAPOD blocks	1.6 (S = 0)	3.0 (S = 1.5)
Grooved CUBES	1.4 (S = 0)	2.7 (S = 2.0)
ACCROPODE®	3.7 (S = 0)	4.1 (S = 0.5)

A comparison of results at a 1% damage level seems interesting even though it may be a little caricatural. The value of 1% was chosen as a kind of average between start of damage and failure: for armour layers consisting of this kind of block, it might be considered as an acceptable damage level.

EFFECT OF DIRECTIONAL SPREADING WITH $\theta = 0°$ referred to test A with monodirectional waves		
Increase of $H_s / \Delta D_n$ at 1% damage level		
Block	$\sigma = 10 - 15°$	$\sigma = 20°$
ROCK	0% to +60%	+90%
TETRAPOD blocks	+15% to +140%	+140%
Grooved CUBES	0% to +20%	+60%
ACCROPODE® blocks	About 0%	Over +20%

EFFECT OF OBLIQUITY WITH $\sigma = 20°$ referred to test E with frontal waves		
Decrease of $H_s / \Delta D_n$ at 1% damage level		
Block	$\theta = 30°$	$\theta = 45°$
ROCK	-20%	-35%
TETRAPOD blocks	-20%	-30%
Grooved CUBES	-25%	-30%
ACCROPODE® blocks	Over -25%	-

Hence, the general trends appear to be:

. Larger spreading yields a more stable situation in the case of frontal waves;

. Larger obliquity yields a more unstable situation in the case of wide spreading.

It may be noted that the ACCROPODE® is fairly stable in all tests (Figure 6): the critical value of $H_s / \Delta D_n$ for start of damage may be estimated between 3.0 and 4.0 depending on wave incidence and spreading*.

Furthermore, ACCROPODE® blocks did not move at all during test E (even at the highest value $H_s / \Delta D_n = 4.5$ reached during the test), neither did they move during test F (maximum $H_s / \Delta D_n = 4.0$). This seems to indicate that this block becomes more stable with a wider spreading (test E with $\sigma = 21°$) and with a larger wave incidence (test F with $\theta = 45°$).

* Van der Meer's estimate for monodirectional frontal waves is 3.7 and SOGREAH's design value including a safety factor is 2.5 for breaking waves and 2.7 for non-breaking waves.

3.2 WAVE OVERTOPPING

During each of the 8 wave height steps, the number of overtopping waves was counted (Nov) and related to the total number of waves (Nt) to be expressed as a percentage in Figures 7 and 8, where all results were plotted into one graph per type of block as a function of $(R_c/H_s)S_{op}^{1/3}$ (R_c : crest elevation above SWL, 140 mm in all tests).

No general trends related to directional spreading and/or wave incidence have been detected so far. All types of block seem to behave rather similarly with:

- Almost no overtopping or $(R_c/H_s)S_{op}^{1/3} > 0.5$;
- Many waves overtopping for $(R_c/H_s)S_{op}^{1/3} < 0.3$.

3.3 WAVE REFLECTION

Although this was not a specific objective of this study, it was decided to perform a brief literature study on this subject and to plot the results of the present tests together with other data.

It was found that some researchers use a fictitious wave steepness consisting of a nearshore wave height combined with an offshore wave length which in fact stands for the (square of the) wave period. On the other hand, some researchers have decided to present their data as a function of the nearshore wave steepness included in the surf similarity parameter (ξ) :

$$\xi_p = tg\ \alpha\ /\ \sqrt{H_s/L_p}$$

where the index "p" relates to the peak period used for computing the nearshore wave length L_p according to the linear theory.

All data collected is shown in Figure 9 for the four types of block and it appears that, for $\xi_p < 6$, linear relations exist between the reflection coefficient Cr and ξ_p. However, the scatter is quite large.

The following notes are made:

- It appears from Allsop's data that smooth slopes are twice as reflective as rock slopes (for $\xi_m < 4$) and that the present tests fit the trend;
- The present tests also fit Oumeraci's data very well for Tetrapod blocks (Oumeraci's data were deduced form large-scale tests);
- Data on grooved cubes was found in LCHF's archives and shows rather low reflection coefficients. However, randomly placed cubes tend to get paved after some storms and the reflection then dramatically increases as was shown in the present tests;

- Data on ACCROPODE® blocks was found in SOGREAH's archives and in Muttray/Oumeraci's latest publication on large-scale tests. It appears that these results show smaller reflection coefficients than SOGREAH's small-scale tests.

  Furthermore, the influence of the sea bed slope in front of the structure does not seem to be very great.

It also appeared during the present tests that a large overtopping percentage yields a lower reflection coefficient.

4. CONCLUSIONS

The following conclusions are drawn from this study:

4.1 ARMOUR STABILITY

- Armour stability increases with increasing directional spreading in most cases with frontal waves;
- Armour stability decreases with increasing obliquity in all cases with wide directional spreading;
- In all tests the critical value of $H_s/\Delta D_n$ for ACCROPODE® ranged between 3.0 and 4.0 or more;
- These general trends are preliminary and perhaps even somewhat caricatural; it is therefore a simple matter of prudence to check the stability of coastal structures in a scale model with multidirectional waves when assessing their safety.

4.2 WAVE OVERTOPPING

- No general trends related to directional spreading and/or wave incidence were detected so far for wave overtopping;
- The four types of block investigated seem to behave similarly with almost no overtopping for $(R_c/H_s)S_{op}^{1/3} > 0.5$ and many waves overtopping for $(R_c/H_s)S_{op}^{1/3} < 0.3$.

4.3 WAVE REFLECTION

- The data on reflection coefficients yield linear relationships with ξ_p (for $\xi_p < 6$) if ξ_p is based on the local wave length;
- The reflection coefficients decrease with increasing overtopping, and paving of cubes produces a large increase in the reflection coefficient.

5. ACKNOWLEDGMENTS

This work was undertaken as part of the MAST G6 Coastal Structures Research Programme. It was funded jointly by SOGREAH's own R/D funds, by Service Technique Central des Ports Maritimes et des Voies Navigables, and by the Commission of the European Communities Directorate General for Science, Research and Development under contract n° MAST 0035C.

6. REFERENCES

ALLSOP N.W.H. (1990) : "Reflection performance of rock armoured slopes in random waves". Proc. ICCE, Delft.

CUR/CIRIA (1991) : "Manual on the use of rock in coastal and shoreline engineering", CUR report n° 154 / CIRIA special publication n° 83.

GILBERT G. and HUNTINGTON S.W. (1991) : "A technique for the generation of short crested waves in wave basins", J. of Hyd. Res., vol. 29, n° 6, pp. 789-799.

van der MEER J. W. (1989) : "Measurement and analysis of directional seas in a basin". Proc. IAHR Conference, Ottawa.

MITSUYASU H. et al (1975) : "Observations of the directional spectrum using a cloverleaf buoy". Journal of Physical Oceanography, Vol. 5.

MUTTRAY M. et al (1992) : "Wave energy dissipation on and in rubble mound structures". Proc. ICCE, Venice.

NWOGU O.U., MANSARD E.P.D., MILES M.D. and ISAACSON M. (1987) : "Estimation of directional wave spectra by the Maximum Entropy method". Proc. IAHR seminar on wave analysis and generation in laboratory basins, Lausanne.

OUMERACI H., PARTENSCKY H.W. (1990) : "Wave-induced pore pressure in rubble mound breakwaters". Proc. ICCE, Delft.

SAND S.E. and MYNETT A.E. (1987) : "Directional wave generation and analysis". Proc. IAHR seminar on wave analysis and generation in laboratory basins, Lausanne.

-

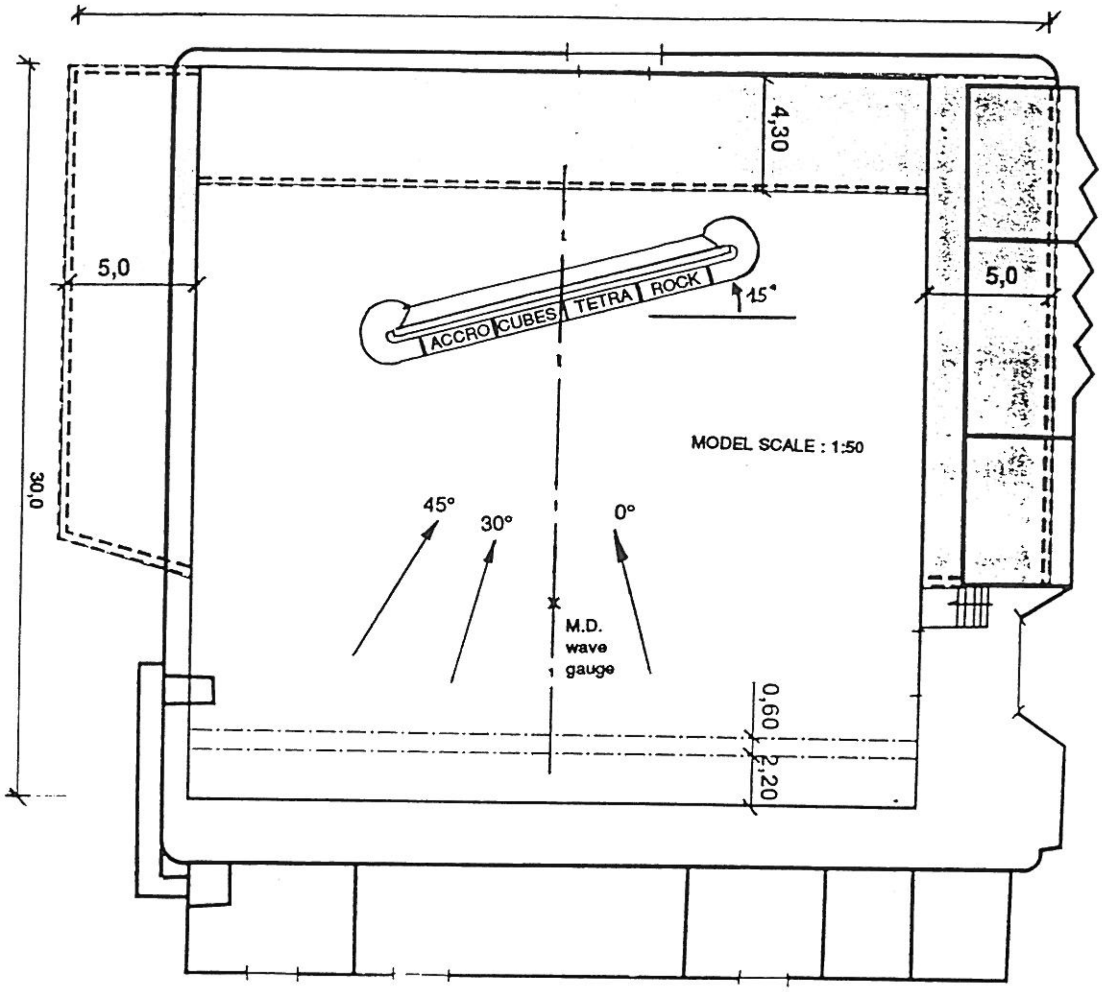

Figure 1

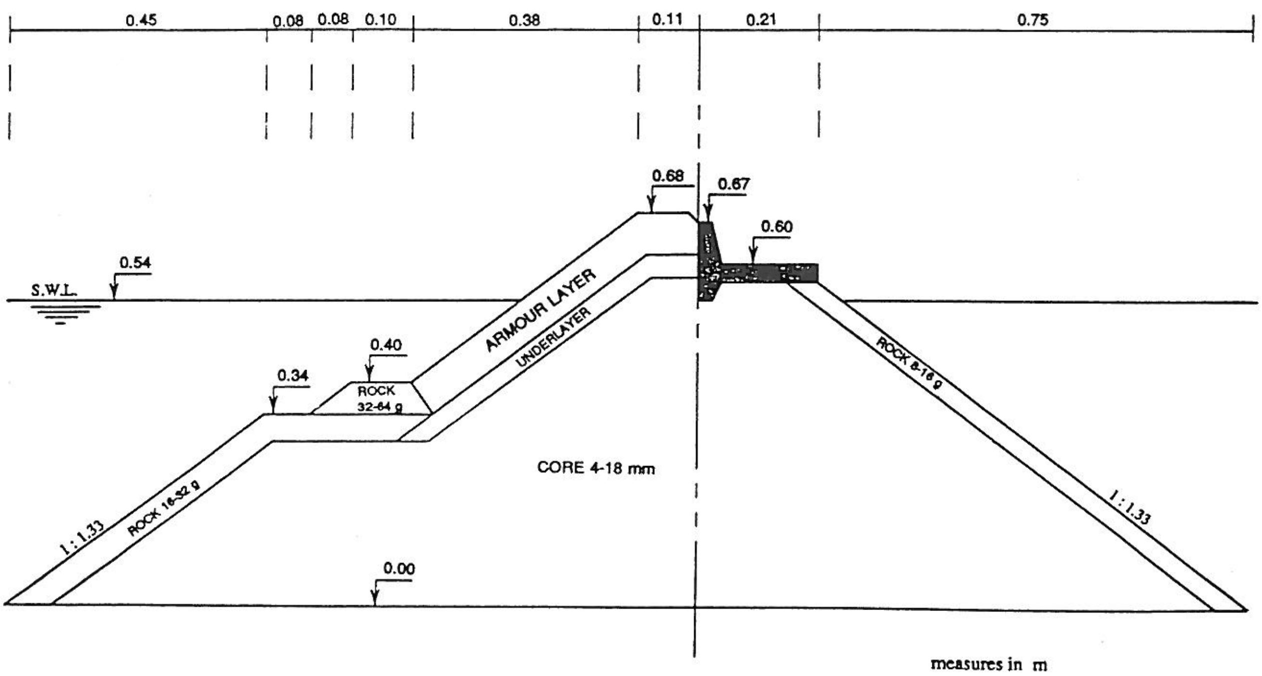

Figure 2

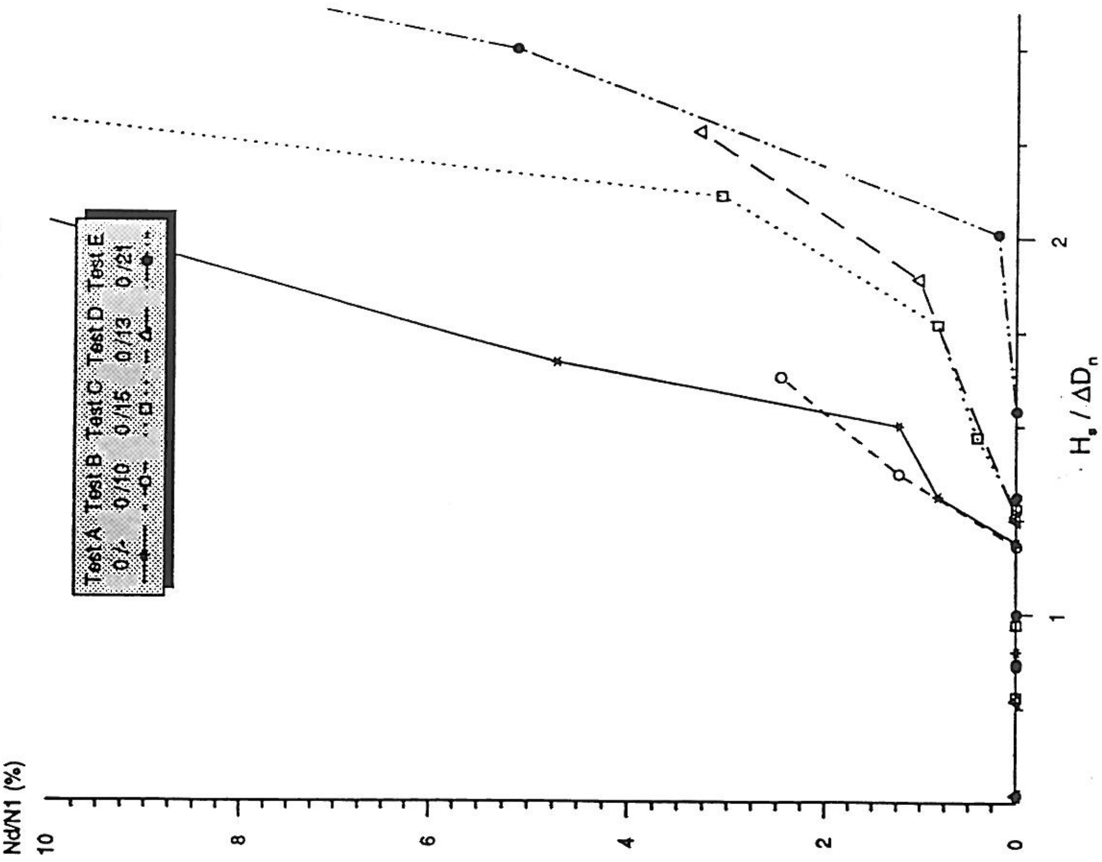

ARMOUR STABILITY - ROCK
Test A Test B Test C Test D Test E
0/- 0/10 0/15 0/13 0/21
Nd/N1 (%)
10
8
6
4
2
0
1
2
H_s / ΔD_n

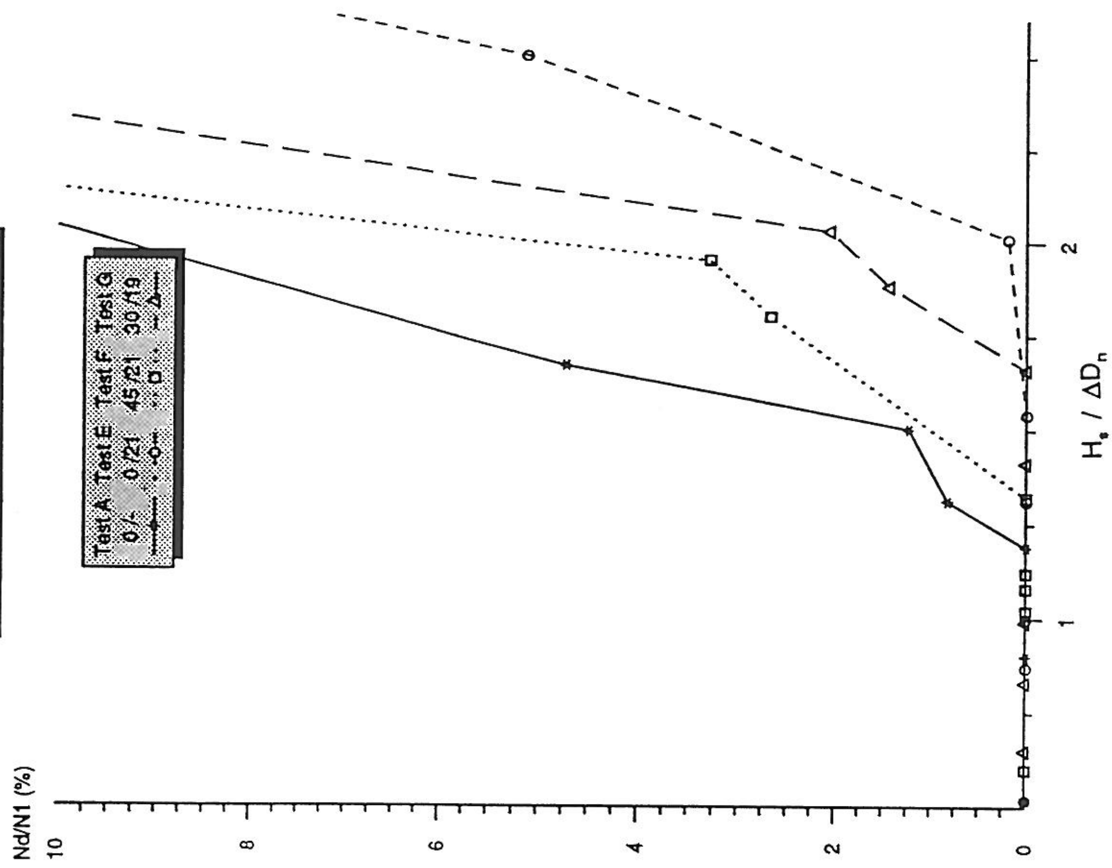

ARMOUR STABILITY - ROCK
Test A Test E Test F Test G
0/- 0/21 45/21 30/19
Nd/N1 (%)
10
8
6
4
2
0
1
2
H_s / ΔD_n

Figure 3

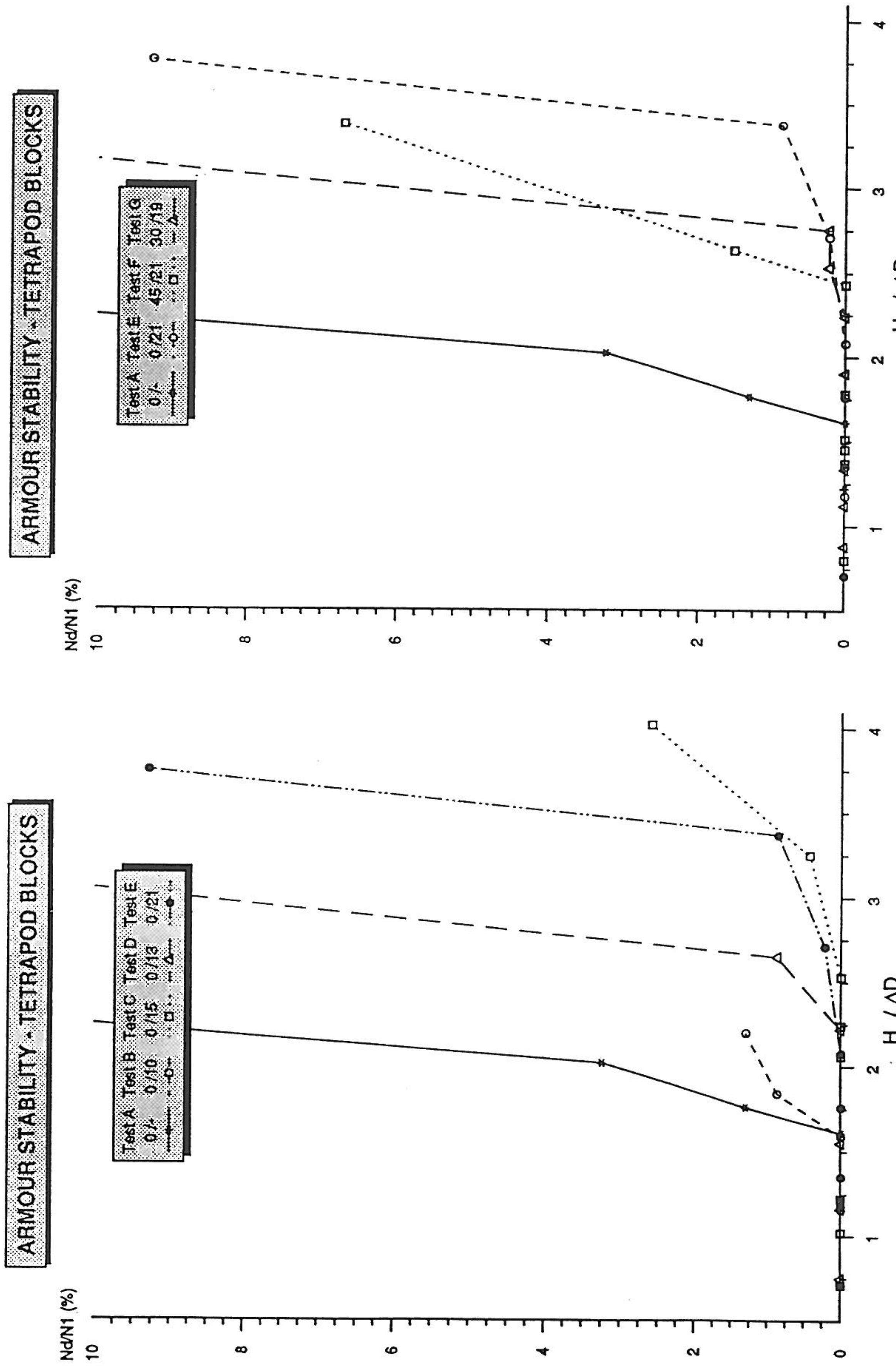
ARMOUR STABILITY - TETRAPOD BLOCKS
Test A Test B Test C Test D Test E
0/- 0/10 0/15 0/13 0/21
Nd/N1 (%)
H_s / ΔD_n
ARMOUR STABILITY - TETRAPOD BLOCKS
Test A Test E Test F Test G
0/- 0/21 45/21 30/19
Nd/N1 (%)
H_s / ΔD_n

Figure 4

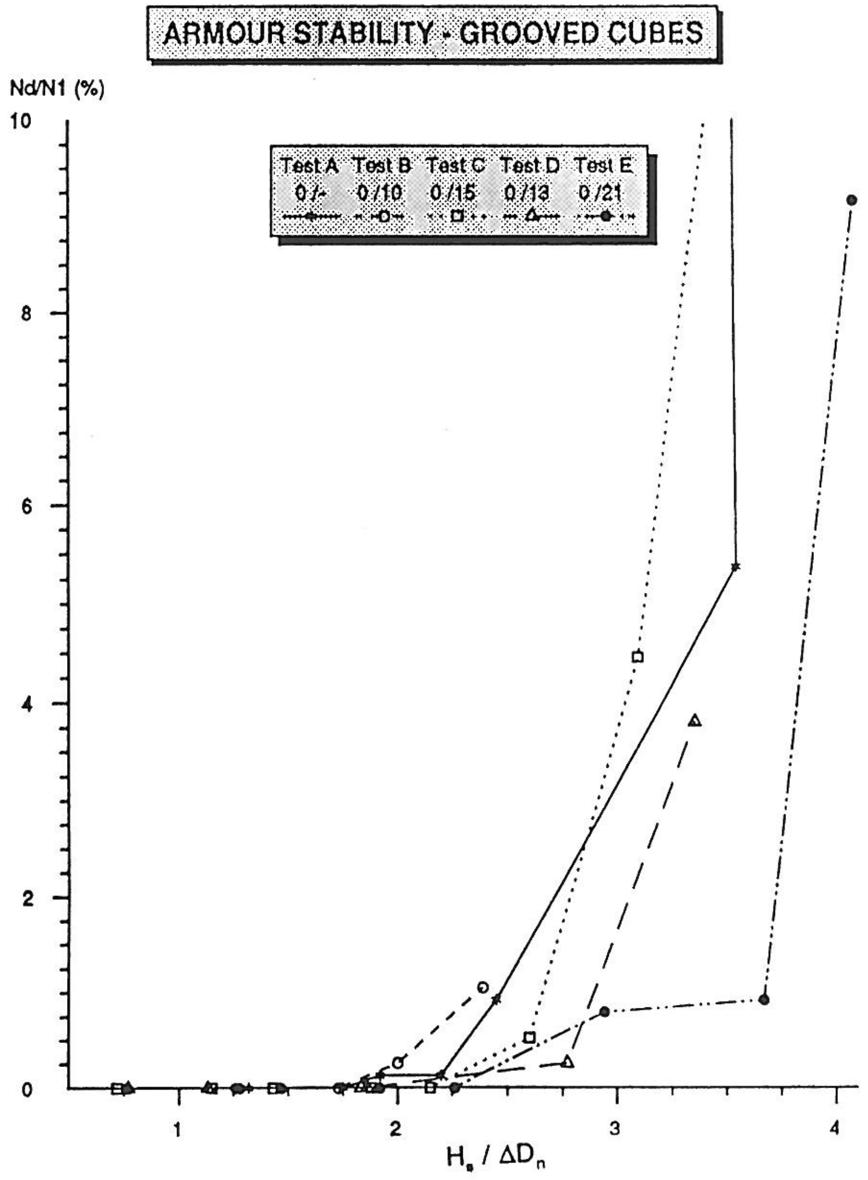
ARMOUR STABILITY - GROOVED CUBES
Nd/N1 (%)
Test A Test B Test C Test D Test E
0/- 0/10 0/15 0/13 0/21
H_s / ΔD_n

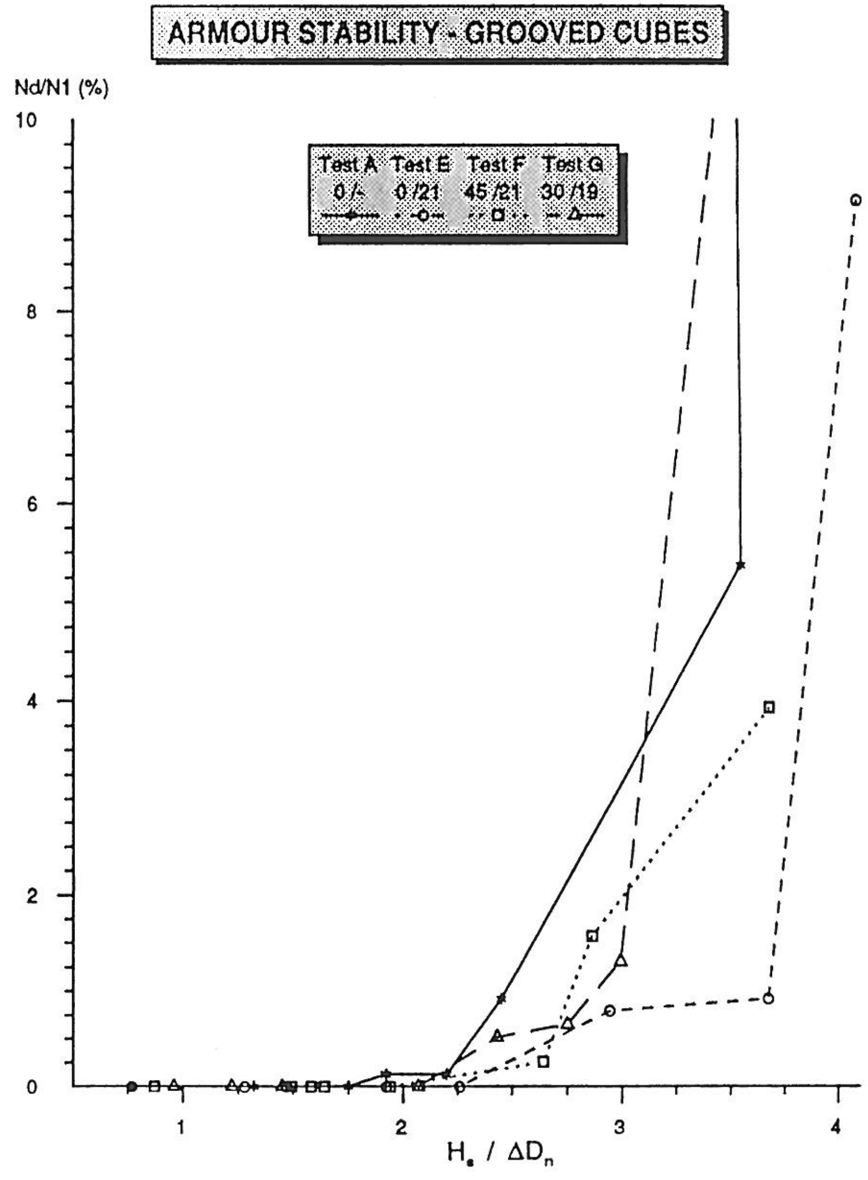
ARMOUR STABILITY - GROOVED CUBES
Nd/N1 (%)
Test A Test E Test F Test G
0/- 0/21 45/21 30/19
H_s / ΔD_n

Figure 5

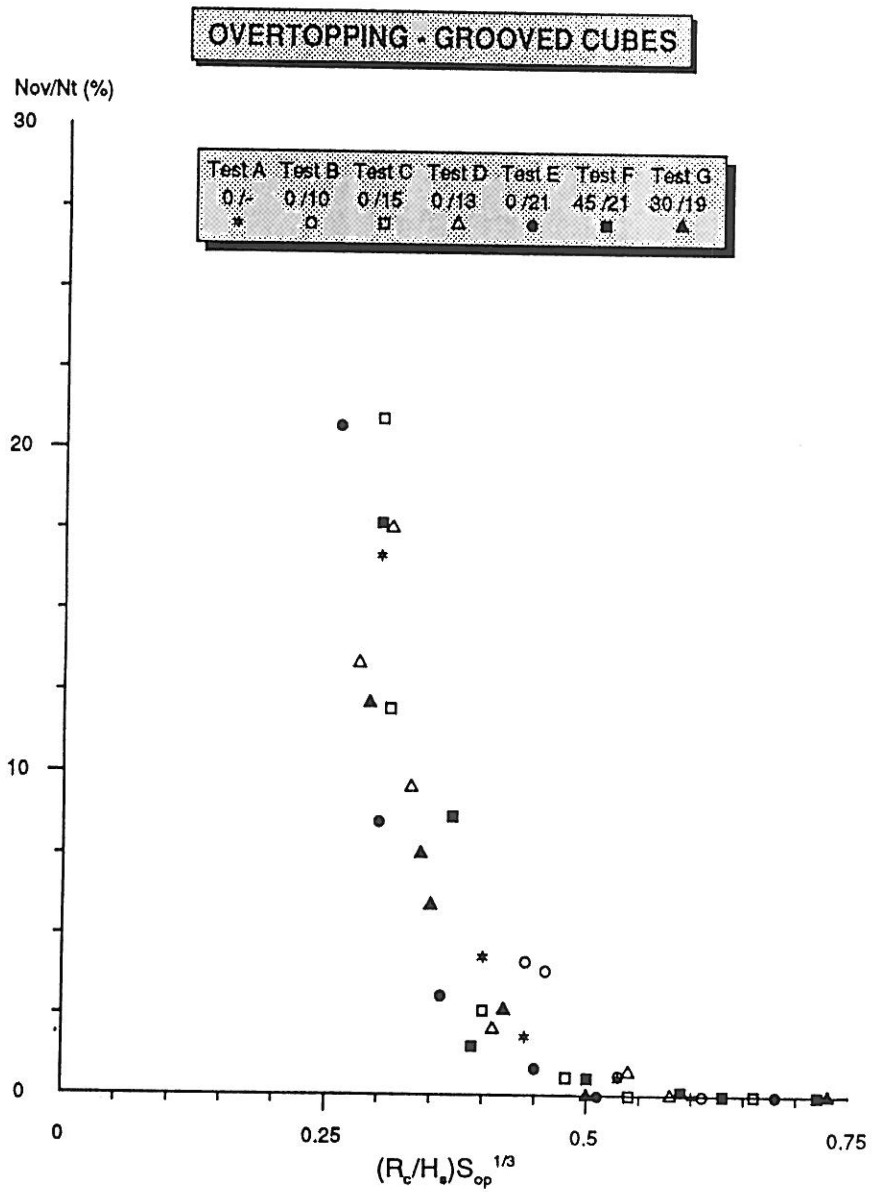

OVERTOPPING - GROOVED CUBES
Nov/Nt (%)
Test A 0/- Test B 0/10 Test C 0/15 Test D 0/13 Test E 0/21 Test F 45/21 Test G 30/19
$(R_c/H_s)S_{op}^{1/3}$
0
10
20
30
0.25
0.5
0.75

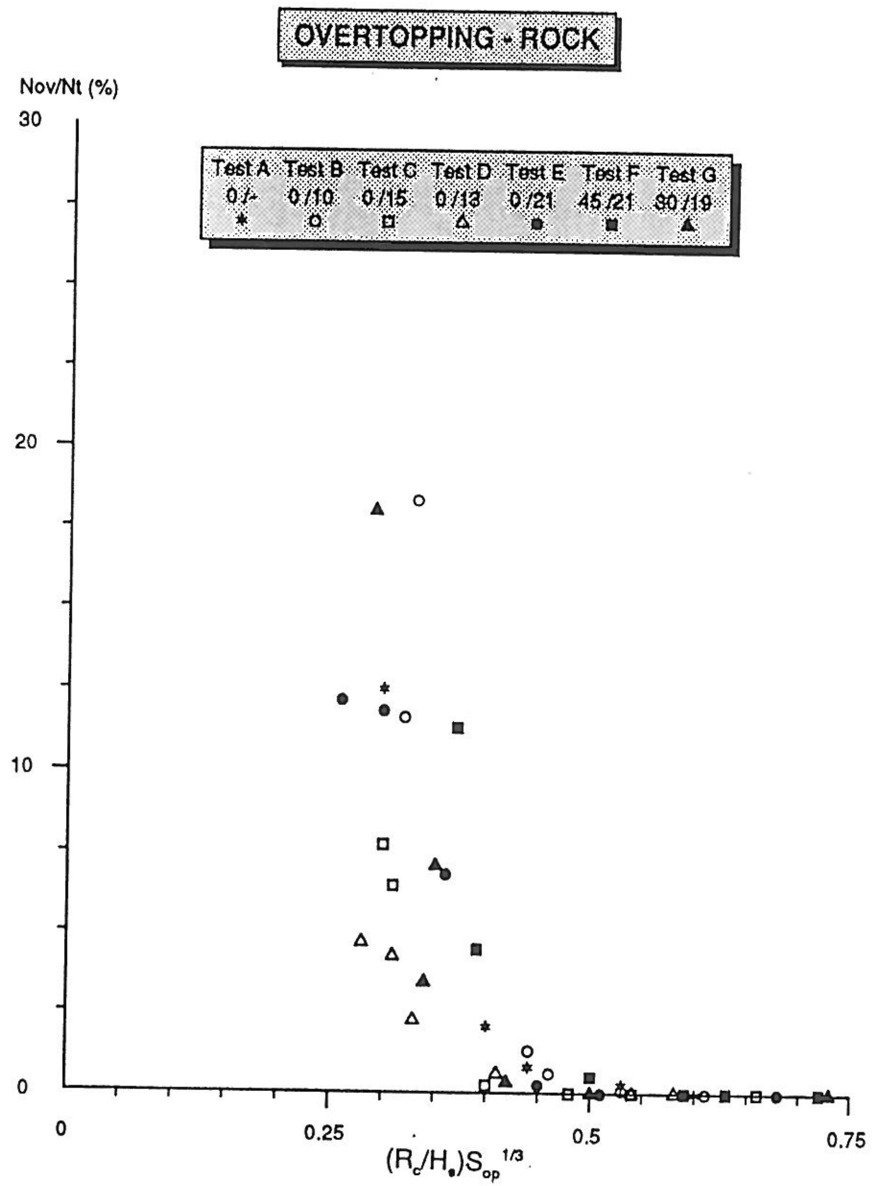

OVERTOPPING - ROCK
Nov/Nt (%)
Test A 0/- Test B 0/10 Test C 0/15 Test D 0/13 Test E 0/21 Test F 45/21 Test G 30/19
$(R_c/H_s)S_{op}^{1/3}$
0
10
20
30
0.25
0.5
0.75

Figure 7

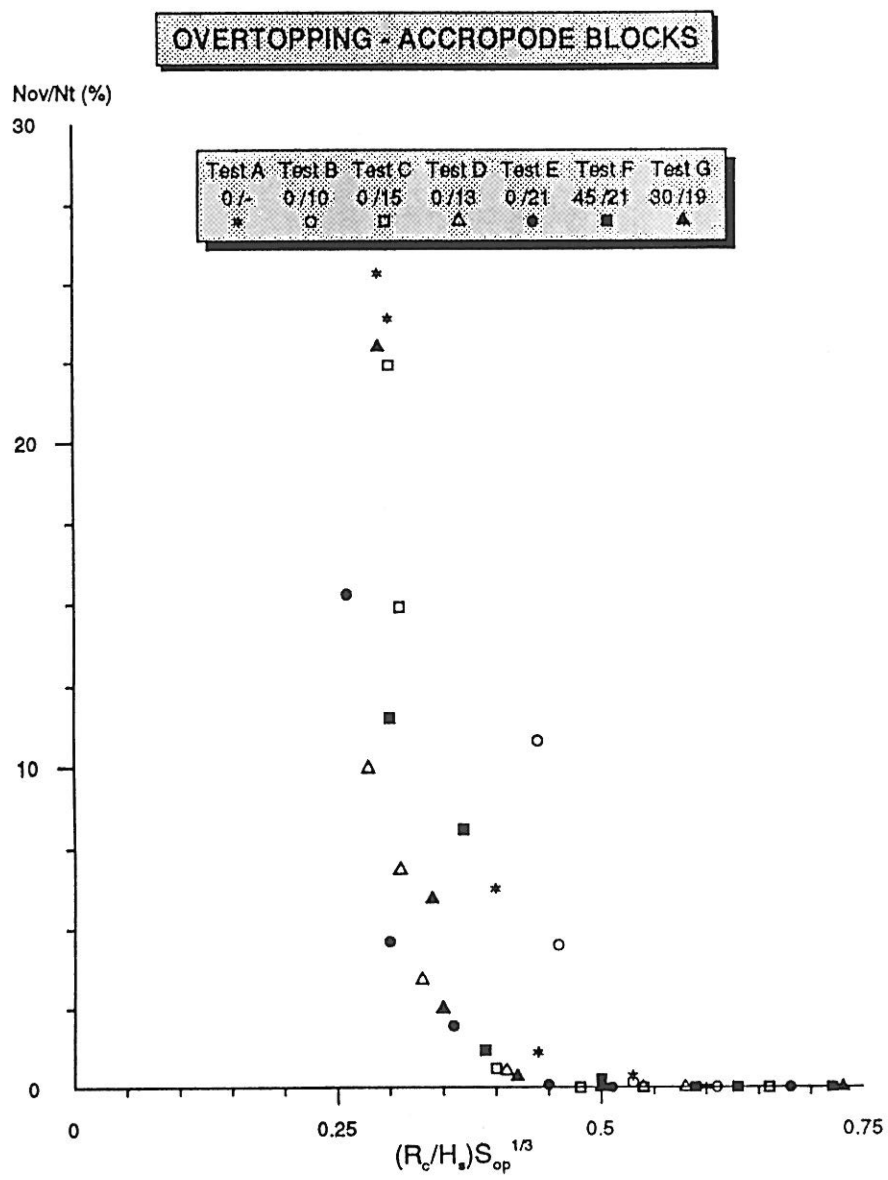
OVERTOPPING - ACCROPODE BLOCKS
Nov/Nt (%)
30
20
10
0
Test A 0/- *
Test B 0/10
Test C 0/15
Test D 0/13
Test E 0/21
Test F 45/21
Test G 30/19
0
0.25
0.5
0.75
$(R_c/H_s)S_{op}^{1/3}$

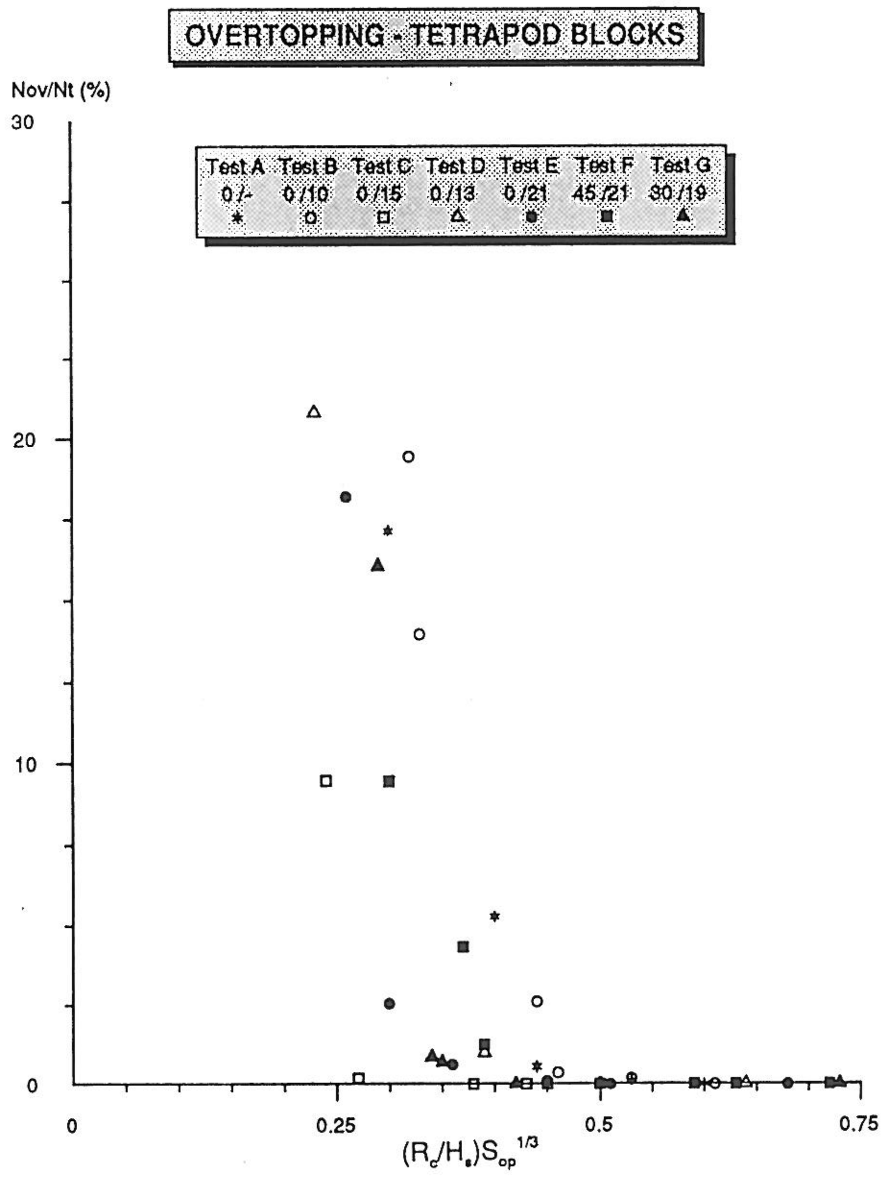
OVERTOPPING - TETRAPOD BLOCKS
Nov/Nt (%)
30
20
10
0
Test A 0/- *
Test B 0/10
Test C 0/15
Test D 0/13
Test E 0/21
Test F 45/21
Test G 30/19
0
0.25
0.5
0.75
$(R_c/H_s)S_{op}^{1/3}$

Figure 8

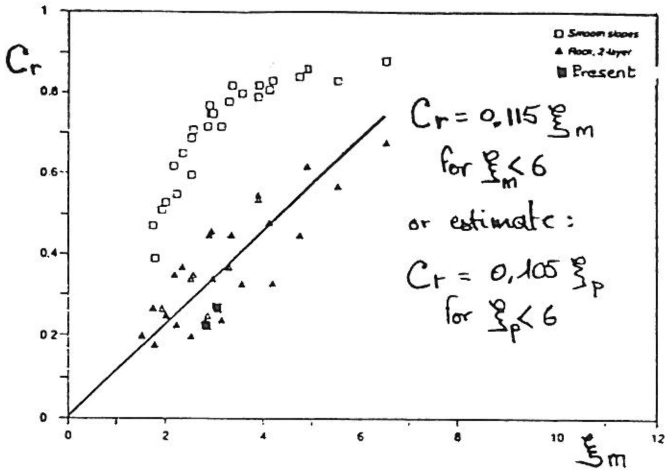

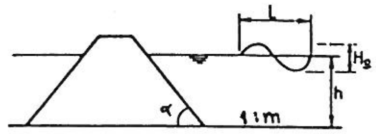

$Cr = Hi/Hr$

$\xi_p = tg\,\alpha / \sqrt{H_s / L_p}$

$\xi_m = tg\,\alpha / \sqrt{H_s / L_m}$

ROCK
Data from Allsop 1990

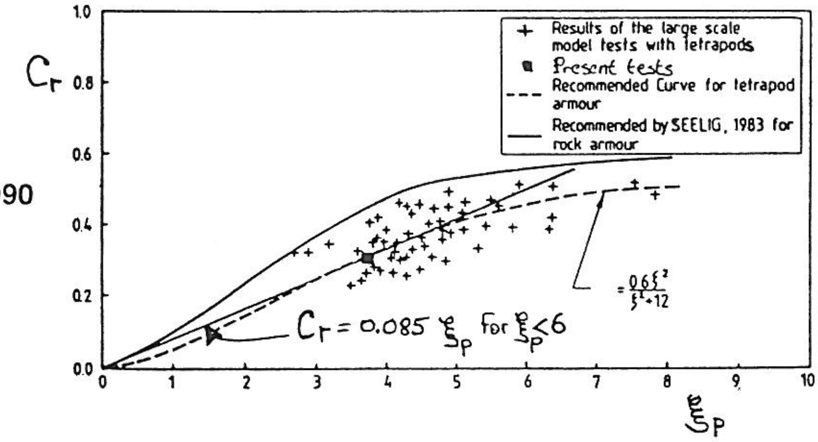

TETRAPOD BLOCKS
Data from Oumeraci 1990

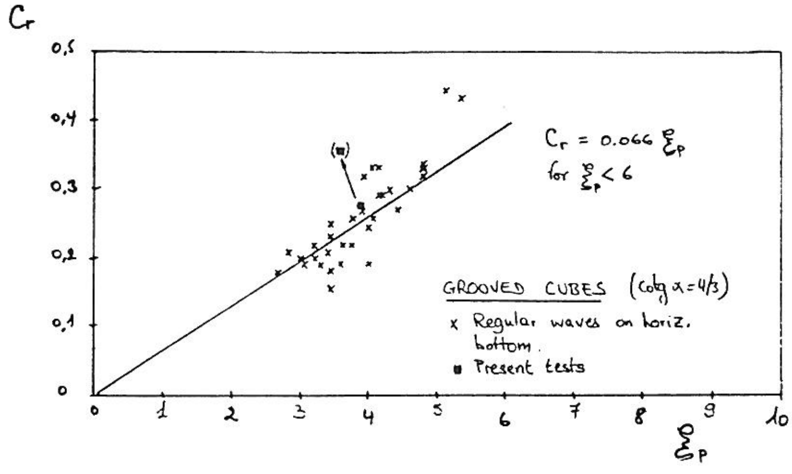

UNPAVED
GROOVED CUBES
Data from LCHF 1983

ACCROPODE BLOCKS
Data from SOGREAH 1983
and Oumeraci 1992

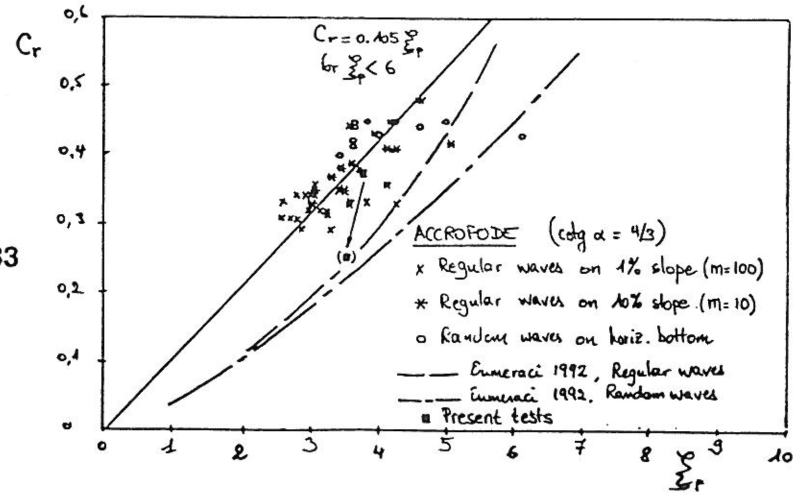

reflection coefficients **Figure 9**